STEADY-STATE ANALYSIS OF A SEMI-BLIND ADAPTIVE BEAMFORMING ALGORITHM FOR TDMA SIGNALS

Myung-Hoon Yeon and John J. Shynk

Department of Electrical and Computer Engineering
University of California, Santa Barbara, CA 93106-9560 USA

ABSTRACT

We describe an adaptive beamforming algorithm for time-division multiple-access (TDMA) signals that utilizes a modified least-squares (LS) cost function, and analyze its performance using a stochastic model. The beamformer weights are computed via a two-step procedure: initial weights are calculated from the training sequence, and these are refined by a semi-blind algorithm using the modified LS cost function. The main goal of the paper is to analyze this algorithm using a stochastic model and Wiener filter theory for the case when the look-direction vector is mismatched. The performance of the proposed adaptive beamformer is also evaluated using simulated TDMA data.

Index Terms— Array signal processing, least-squares methods, interference suppression, time-division multiaccess.

1. INTRODUCTION

In cellular radio systems, signals transmitted in one cell can interfere with those in other cells that use the same frequencies. We investigate an adaptive beamforming receiver that is designed to suppress this cochannel interference (CCI) in a TDMA system. Usually, the adaptive beamformer weights are calculated using only the known training sequence contained in each TDMA slot (burst). However, the CCI affecting the coded data could differ significantly from that during the training sequence. In an effort to solve this problem, the equalizer output could be combined with the original training sequence to construct an extended training sequence for the beamformer [1]. A modified burst-based LS estimator with projections was proposed in [2], and a regularized LS algorithm for constant modulus (CM) signals was described in [3]; however, both of these approaches have a high computational complexity. Compared to previous work, the proposed semi-blind algorithm is quite simple as well as practical because of the LS approximation used for the CM signals [4].

In the iterative receiver, the beamformer weights are updated using the semi-blind algorithm in a multistage architecture as shown in Figure 1. In the first stage, the initial beamformer weights are computed using the known training sequence, and these are refined using an extended training sequence in the semi-blind algorithm. In the second stage, the initial beamformer weights are computed using re-encoded data, and then a semi-blind algorithm compensates for weight distortions caused by errors in the re-encoded data. For the stochastic analysis, we assume BPSK signals and employ Wiener filter theory. We assume that the look-direction vector is not precisely known, i.e., it has an error component and thus is mismatched [5].

2. SUMMARY OF THE ITERATIVE SEMI-BLIND BEAMFORMING ALGORITHM

In the first stage of the algorithm, the beamformer weights are calculated using a two-step procedure. First, initial beamformer weights $\mathbf{w}_0$ are computed by minimizing the LS cost function $J_0(\mathbf{w}_0) = \sum_{k=0}^{m-1} |\mathbf{w}_0{}^H \mathbf{x}(k) - t_b(k)|^2$ where t_b is the known training sequence of length m, the subscript b denotes the beamformer, the (column) vector $\mathbf{x}$ contains the array data, and the superscript H denotes complex conjugate transpose. Second, the refined beamformer weights $\mathbf{w}_1$ are computed by minimizing

$$J_1(\mathbf{w}_1) = \sum_{k=0}^{m-1} |\mathbf{w}_1^H \mathbf{x}(k) - t_b(k)|^2 + \sum_{k=m}^{j-1} |\mathbf{w}_1^H \mathbf{z}_0(k) - 1|^2 \tag{1}$$

where $j - m$ is the length of the coded data. The LS cost function for CM signals was modified in order to generate the semi-blind algorithm: $J(\mathbf{w}_1) = \sum_{k=m}^{j-1} (|\mathbf{w}_1^H \mathbf{x}(k)|^2 - 1)^2 = \sum_{k=m}^{j-1} (\mathbf{w}_1^H \mathbf{x}(k)\mathbf{x}^H(k)\mathbf{w}_1 - 1)^2 \approx \sum_{k=m}^{j-1} (\mathbf{w}_1^H \mathbf{x}(k)\mathbf{x}^H(k)\mathbf{w}_0 - 1)^2 = \sum_{k=m}^{j-1} (\mathbf{w}_1^H \mathbf{z}_0(k) - 1)^2$ where $\mathbf{z}_0(k) \triangleq \mathbf{x}(k)\mathbf{x}^H(k)\mathbf{w}_0$. Note that we have exploited the approximation $\mathbf{x}^H(k)\mathbf{w}(n) \approx \mathbf{x}^H(k)\mathbf{w}(k-1)$ when k is close to n [6]. In the second stage, the initial beamformer weights $\mathbf{w}_2$ are computed using re-encoded data, and then are refined to generate $\mathbf{w}_3$ using the following semi-blind cost function:

$$J_2(\mathbf{w}_3) = \sum_{k=m}^{j-1} |\mathbf{w}_3^H \mathbf{x}(k) - t_{br}(k-m)|^2 + \sum_{k=m}^{j-1} |\mathbf{w}_3^H \mathbf{z}_2(k) - 1|^2 \tag{2}$$

where $\mathbf{z}_2(k) \triangleq \mathbf{x}(k)\mathbf{x}^H(k)\mathbf{w}_2$ and t_{br} are the re-encoded data for the beamformer.

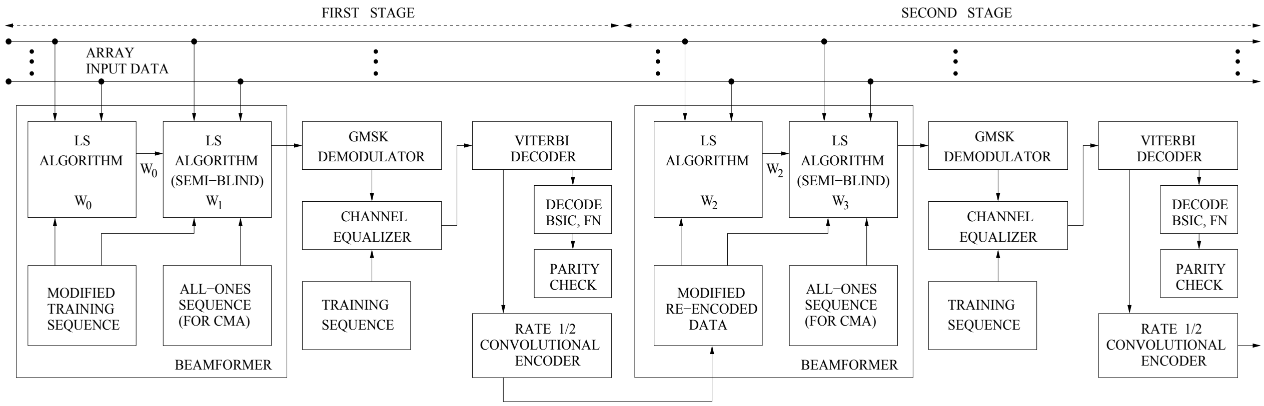

Fig. 1. Multistage receiver using the semi-blind beamformer.

3. STOCHASTIC ANALYSIS

We assume that one desired BPSK signal b_1 and two interfering BPSK signals b_2 and b_3 arrive at a two-element array as shown in Figure 2. b_1 consists of a known training sequence and coded data, b_2 is interference during the training sequence of b_1, and b_3 is interference during the coded data of b_1. At the two antenna elements, the received signals $\mathbf{x}_t$ in the region of the training sequence of b_1 are represented by $\mathbf{x}_t = [x_{t1}, x_{t2}]^T$, and those in the region of the coded data of b_1 are given by $\mathbf{x}_d = [x_{d1}, x_{d2}]^T$. Thus, $x_{t1} = b_1 + b_2 + n_1$, $x_{t2} = b_1 e^{j\theta_1} + b_2 e^{j\theta_2} + n_2$, $x_{d1} = b_1 + b_3 + n_3$, and $x_{d2} = b_1 e^{j\theta_1} + b_3 e^{j\theta_3} + n_4$ where the subscripts t and d denote the training sequence and coded data in a slot, respectively. The $\{b_i\}$ are independent and identically distributed with alphabet $\{-1, 1\}$, and thus have zero mean and unit variance, i.e., $E[b_i b_j] = \delta_{ij}$. The additive noise n_i is white and Gaussian with zero mean and variance σ_n^2, i.e., $E[n_i n_j^*] = \sigma_n^2 \delta_{ij}$. The deterministic phase $\theta_i = -2\pi\Delta \cos\phi_i/\lambda$ represents the carrier phase shift across the two antenna elements, where ϕ_i is the angle of incidence, Δ is the interelement spacing, and λ is the wavelength.

The initial beamformer weights $\mathbf{w}_0$ are computed from the Wiener-Hopf equation. Define the correlation matrix $\mathbf{R}_t \stackrel{\Delta}{=} E[\mathbf{x}_t \mathbf{x}_t^H]$ where $\mathbf{x}_t$ was previously specified, and define the cross-correlation vector

$$\mathbf{p}_t \stackrel{\Delta}{=} E[\mathbf{x}_t d_t^*] = E[x_{t1} b_1^* \;\; x_{t2} b_1^*]^T = [1 \;\; e^{j\theta_1}]^T \tag{3}$$

where d_t represents the desired signal, and the superscript * denotes complex conjugation. Let $\mathbf{w}_0 \stackrel{\Delta}{=} [w_{t1}, w_{t2}]^T$ be the initial beamformer weights given by the Wiener solution

$$\mathbf{w}_0 = \mathbf{R}_t^{-1} \mathbf{p}_t. \tag{4}$$

The refined beamformer weights $\mathbf{w}_1$ are computed from $\mathbf{x}_d$ using $\mathbf{w}_0$. Define the vector $\mathbf{z} \stackrel{\Delta}{=} \mathbf{x}_d \mathbf{x}_d^H \mathbf{w}_0$ and partition the correlation matrix as follows:

$$\mathbf{R}_{cd} \stackrel{\Delta}{=} E[\mathbf{z}\mathbf{z}^H] = E \begin{bmatrix} A & B \\ C & D \end{bmatrix} \tag{5}$$

where the subscript cd denotes coded data and

$$\begin{aligned}
E[A] &= w_{t1} E[x_{d1} x_{d1}^* x_{d1} x_{d1}^*] w_{t1}^* + w_{t2} E[x_{d1} x_{d2}^* x_{d1} x_{d1}^*] w_{t1}^* \\
&\quad + w_{t1} E[x_{d1} x_{d1}^* x_{d2} x_{d1}^*] w_{t2}^* + w_{t2} E[x_{d1} x_{d2}^* x_{d2} x_{d1}^*] w_{t2}^* \\
E[B] &= w_{t1} E[x_{d1} x_{d1}^* x_{d1} x_{d2}^*] w_{t1}^* + w_{t2} E[x_{d1} x_{d2}^* x_{d1} x_{d2}^*] w_{t1}^* \\
&\quad + w_{t1} E[x_{d1} x_{d1}^* x_{d2} x_{d2}^*] w_{t2}^* + w_{t2} E[x_{d1} x_{d2}^* x_{d2} x_{d2}^*] w_{t2}^* \\
E[C] &= w_{t1} E[x_{d2} x_{d1}^* x_{d1} x_{d1}^*] w_{t1}^* + w_{t2} E[x_{d2} x_{d2}^* x_{d1} x_{d1}^*] w_{t1}^* \\
&\quad + w_{t1} E[x_{d2} x_{d1}^* x_{d2} x_{d1}^*] w_{t2}^* + w_{t2} E[x_{d2} x_{d2}^* x_{d2} x_{d1}^*] w_{t2}^* \\
E[D] &= w_{t1} E[x_{d2} x_{d1}^* x_{d1} x_{d2}^*] w_{t1}^* + w_{t2} E[x_{d2} x_{d2}^* x_{d1} x_{d2}^*] w_{t1}^* \\
&\quad + w_{t1} E[x_{d2} x_{d1}^* x_{d2} x_{d2}^*] w_{t2}^* + w_{t2} E[x_{d2} x_{d2}^* x_{d2} x_{d2}^*] w_{t2}^*.
\end{aligned} \tag{6}$$

The components are given by

$$\begin{aligned}
E[x_{d1} x_{d1}^* x_{d1} x_{d1}^*] &= 8 + 8\sigma_n^2 + 2\sigma_n^4 \\
E[x_{d1} x_{d2}^* x_{d1} x_{d1}^*] &= 4e^{-j\theta_1} + 4e^{-j\theta_3} + 2e^{-j\theta_1}\sigma_n^2 \\
&\quad + 2e^{-j\theta_3}\sigma_n^2 \\
E[x_{d1} x_{d1}^* x_{d2} x_{d1}^*] &= 4e^{j\theta_1} + 4e^{j\theta_3} + 2e^{j\theta_1}\sigma_n^2 + 2e^{j\theta_3}\sigma_n^2 \\
E[x_{d1} x_{d2}^* x_{d2} x_{d1}^*] &= 4 + 2e^{j(\theta_3 - \theta_1)} + 2e^{j(\theta_1 - \theta_3)} + 4\sigma_n^2 \\
&\quad + 2\sigma_n^4 \\
E[x_{d1} x_{d1}^* x_{d1} x_{d2}^*] &= 4e^{-j\theta_1} + 4e^{-j\theta_3} + 2e^{-j\theta_1}\sigma_n^2 \\
&\quad + 2e^{-j\theta_3}\sigma_n^2 \\
E[x_{d1} x_{d2}^* x_{d1} x_{d2}^*] &= 2e^{-j2\theta_1} + 2e^{-j2\theta_3} + 4e^{-j(\theta_1 + \theta_3)} \\
E[x_{d1} x_{d1}^* x_{d2} x_{d2}^*] &= 4 + 2e^{j(\theta_3 - \theta_1)} + 2e^{j(\theta_1 - \theta_3)} + 4\sigma_n^2 \\
&\quad + 2\sigma_n^4 \\
E[x_{d1} x_{d2}^* x_{d2} x_{d2}^*] &= 3e^{-j\theta_1} + 3e^{-j\theta_3} + e^{j(\theta_3 - 2\theta_1)} \\
&\quad + e^{j(\theta_1 - 2\theta_3)} + 2(e^{-j\theta_1} + e^{-j\theta_3})\sigma_n^2 \\
E[x_{d2} x_{d1}^* x_{d1} x_{d1}^*] &= 4e^{j\theta_1} + 4e^{j\theta_3} + 2e^{j\theta_1}\sigma_n^2 + 2e^{j\theta_3}\sigma_n^2 \\
E[x_{d2} x_{d2}^* x_{d1} x_{d1}^*] &= 4 + 2e^{j(\theta_3 - \theta_1)} + 2e^{j(\theta_1 - \theta_3)} + 4\sigma_n^2 \\
&\quad + 2\sigma_n^4 \\
E[x_{d2} x_{d1}^* x_{d2} x_{d1}^*] &= 2e^{j2\theta_1} + 4e^{j(\theta_1 + \theta_3)} + 2e^{j2\theta_3} \\
E[x_{d2} x_{d2}^* x_{d2} x_{d1}^*] &= 3e^{j\theta_1} + 3e^{j\theta_3} + e^{j(2\theta_1 - \theta_3)} + e^{j(2\theta_3 - \theta_1)} \\
&\quad + 2e^{j\theta_1}\sigma_n^2 + 2e^{j\theta_3}\sigma_n^2
\end{aligned}$$

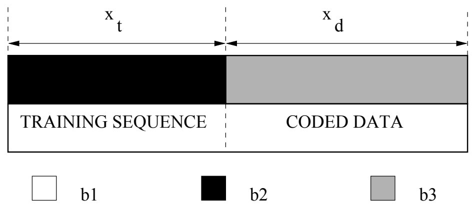

Fig. 2. Scenario for the stochastic analysis.

$$
\begin{aligned}
E[x_{d2}x_{d1}^*x_{d1}x_{d2}^*] &= 4 + 2e^{j(\theta_3-\theta_1)} + 2e^{j(\theta_1-\theta_3)} + 4\sigma_n^2 \\
&\quad +2\sigma_n^4 \\
E[x_{d2}x_{d2}^*x_{d1}x_{d2}^*] &= 3e^{-j\theta_1} + 3e^{-j\theta_3} + e^{j(\theta_3-2\theta_1)} \\
&\quad +e^{j(\theta_1-2\theta_3)} + 2(e^{-j\theta_1} + e^{-j\theta_3})\sigma_n^2 \\
E[x_{d2}x_{d1}^*x_{d2}x_{d2}^*] &= 3e^{j\theta_1} + 3e^{j\theta_3} + e^{j(2\theta_1-\theta_3)} + e^{j(2\theta_3-\theta_1)} \\
&\quad +2e^{j\theta_1}\sigma_n^2 + 2e^{j\theta_3}\sigma_n^2 \\
E[x_{d2}x_{d2}^*x_{d2}x_{d2}^*] &= 6 + e^{j2(\theta_3-\theta_1)} + e^{j2(\theta_1-\theta_3)} + 8\sigma_n^2 \\
&\quad +2\sigma_n^4,
\end{aligned} \tag{7}
$$

which use the following fourth-order moment [7]:

$$E[(x+y)^4] = E[x^4] + E[y^4] + 6E[x^2]E[y^2] \tag{8}$$

where x and y are independent zero-mean random variables. The cross-correlation vector can be rewritten as $\mathbf{p}_{cd} \triangleq E[\mathbf{z}d_d^*]$ $= E[\mathbf{z}] = E[\mathbf{x}_d\mathbf{x}_d^H\mathbf{w}_0]$ where $d_d = 1$ is the fixed modulus (because of the BPSK data).

For the semi-blind algorithm, the input correlation matrix can be expressed as

$$\mathbf{R}_{sb} = E\left[[\mathbf{x}_t \;\; \mathbf{z}]\begin{bmatrix}\mathbf{x}_t^H \\ \mathbf{z}^H\end{bmatrix}\right] = \mathbf{R}_t + \mathbf{R}_{cd} \tag{9}$$

where the subscript sb denotes semi-blind. The corresponding cross-correlation vector is

$$\mathbf{p}_{sb} = E\left[[\mathbf{x}_t \;\; \mathbf{z}]\begin{bmatrix}d_t^* \\ d_d^*\end{bmatrix}\right] = \mathbf{p}_t + \mathbf{p}_{cd}, \tag{10}$$

and the refined beamformer weights are

$$\mathbf{w}_1 = \mathbf{R}_{sb}^{-1}\mathbf{p}_{sb}. \tag{11}$$

In the second stage (shown in Figure 1), $\mathbf{w}_2$ and $\mathbf{w}_3$ are derived using a similar procedure. The initial beamformer weights $\mathbf{w}_2$ are calculated using $\mathbf{x}_d$ instead of $\mathbf{x}_t$. Define the correlation matrix in the second stage as $\mathbf{R}_d \triangleq E[\mathbf{x}_d\mathbf{x}_d^H]$ where $\mathbf{x}_d$ was previously specified. Also, define the cross-correlation vector

$$\mathbf{p}_d \triangleq E[\mathbf{x}_d d_{cd}^*] = E[\mathbf{x}_d b_1^*] = [1 \quad e^{j\theta_1}]^T. \tag{12}$$

Letting $\mathbf{w}_2 \triangleq [w_{d1}, w_{d2}]^T$ be the initial beamformer weights in the second stage, the Wiener weights are given by

$$\mathbf{w}_2 = \mathbf{R}_d^{-1}\mathbf{p}_d. \tag{13}$$

The refined beamformer weights $\mathbf{w}_3$ are computed using $\mathbf{x}_d$ and $\mathbf{w}_2$ (all steps are similar to those in the derivation for $\mathbf{w}_1$ in the first stage). Thus, using the statistics for this scenario, we have derived closed-form expressions for the Wiener weights – including those for the semi-blind algorithm.

4. COMPUTER SIMULATIONS

4.1. Stochastic Model

We evaluate the performance of the semi-blind beamformer using the stochastic model for the scenario in Figure 2. In the first stage, the simulation steps were as follows: (i) Calculate the beamformer weights $\mathbf{w}_0$ in (4) and $\mathbf{w}_1$ in (11). The angles of arrival (AOAs) for b_1, b_2, and b_3 were 60°, 90°, and 150°, respectively. (ii) 10^6 independent samples of $\mathbf{x}_d$ were generated and processed by the beamformers using the Wiener weights. (iii) The bit error rate (BER) was measured at the beamformer output. Figure 3 shows that the semi-blind algorithm improves the performance of the beamformer because it more effectively suppresses the CCI affecting the coded data of b_1. The performance of the semi-blind beamformer using the LS method in Figure 1 is also examined; observe that the BER results are similar to that predicted using the Wiener weights.

In the second stage, since the re-encoded data could include bit errors, the cross-correlation vector $\mathbf{p}$ might be distorted (i.e., look-direction vector mismatch). In the stochastic model, the distorted cross correlation vector can be represented by $\hat{\mathbf{p}}_d = \mathbf{p}_d + \boldsymbol{\beta}$ where $\mathbf{p}_d$ is defined in (12) and $\boldsymbol{\beta}$ models the cross-correlation distortion [5]. We assume that $\boldsymbol{\beta}$ is inversely proportional to the signal-to-noise ratio (SNR) in order to quantify the effects of the re-encoded data errors. The simulation steps were as follows: (i) Calculate the beamformer weights $\mathbf{w}_2$ in (13) and $\mathbf{w}_3$. Note that $\mathbf{w}_2$ and $\mathbf{w}_3$ are computed using $\hat{\mathbf{p}}_d$ instead of $\mathbf{p}_d$ in (12). The AOAs for b_1, b_2, and b_3 were 60°, 90°, and 150°, respectively. (ii) 1000 independent samples of $\mathbf{x}_d$ were generated and processed by the beamformer. (iii) Repeat steps (i) and (ii) for 1000 independent trials. Figure 4 shows that the semi-blind algorithm improves the performance of the beamformer, even though the initial beamformer weights are distorted. This is achieved because the semi-blind beamformer weights are computed not only by using re-encoded data, but also by incorporating the CM component to compensate for the effects of errors in the re-encoded data.

4.2. Simulated TDMA Data

We also verified the multistage semi-blind beamformer in Figure 1 using synchronization channel (SCH) data for the Global System for Mobile (GSM) communications. The SCH channel coding structure is relatively simple and does not require additional complexity (e.g., the interleaving in the

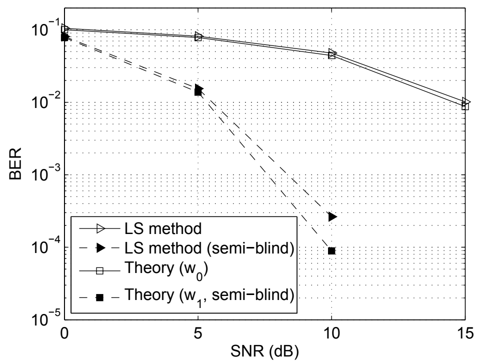

Fig. 3. Stochastic analysis for the first stage.

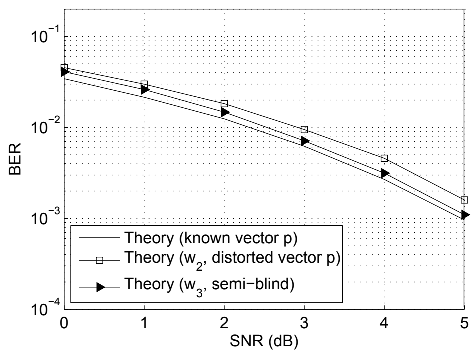

Fig. 4. Stochastic analysis for the second stage.

traffic channel coding). Laurent's decomposition [8] was employed to detect the Gaussian minimum-shift keying (GMSK) signals. A four-element antenna array and four stages were used in the simulations. One desired signal and two interfering signals impinged on the antenna array with random angles in the range $[0°, 180°]$. The sampling interval of the transmitted signals was $T_b/8$, and that of the received array data was T_b (the bit duration). Figure 5 shows that re-encoded data improves the performance of the beamformer in the first few stages. Furthermore, the semi-blind algorithm enhances the performance of the beamformer, and improves the BER performance of the decoder.

5. CONCLUSION

We have presented a semi-blind beamforming algorithm for TDMA signals using a modified LS cost function, and analyzed its performance via a stochastic model, including the case where there is look-direction vector mismatch. In the first stage, the semi-blind algorithm improves the performance of the beamformer because it suppresses the CCI affecting the coded data. In the second stage, this algorithm compensates for the initial weight distortion caused by the look-direction vector mismatch; the all-ones "training" sequence for the CM blind adaptation compensates for errors in the re-encoded data.

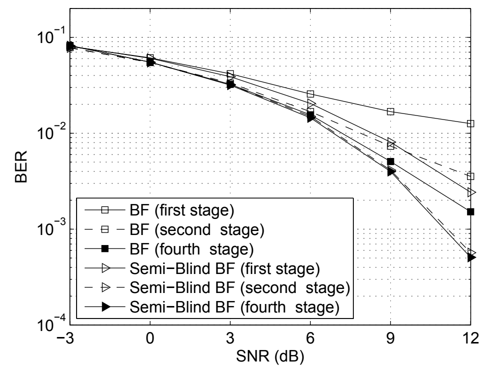

Fig. 5. BER performance of the semi-blind beamformer.

6. ACKNOWLEDGMENT

This work was supported by Applied Signal Technology, Inc., and the University of California MICRO Program.

7. REFERENCES

[1] M. C. Wells, "Increasing the capacity of GSM cellular radio using adaptive antennas," *IEE Proceedings – Communications*, vol. 143, pp. 304–310, Oct. 1996.

[2] A. M. Kuzminskiy and C. B. Papadias, "Re-configurable semi-blind cancellation of asynchronous interference with an antenna array," in *Proc. IEEE Int. Conf. on Acoustics, Speech, Signal Processing*, vol. 4, Hong Kong, Apr. 2003, pp. 696–699.

[3] A. M. Kuzminskiy and D. Hatzinakos, "Semi-blind training-like estimation of spatio-temporal filter coefficients for finite alphabet signals," in *Proc. IEEE SP Workshop on Statistical Signal and Array Processing*, Portland, OR, Sep. 1998, pp. 376–379.

[4] M. H. Yeon, J. J. Shynk, and R. P. Gooch, "A semi-blind adaptive GSM beamformer using re-encoded data," in *Proc. Forty-First Conf. on Information Sciences and Systems*, Baltimore, MD, Mar. 2007.

[5] S. A. Vorobyov, A. B. Gershman, and Z.-Q. Luo, "Robust adaptive beamforming using worst-case performance optimization: A solution to the signal mismatch problem," *IEEE Trans. Signal Processing*, vol. 51, pp. 313–324, Feb. 2003.

[6] Y. Chen, T. Le-Ngoc, B. Champagne, and C. Xu, "Recursive least squares constant modulus algorithm for blind adaptive array," *IEEE Trans. Signal Processing*, vol. 52, pp. 1452–1456, May 2004.

[7] A. Teschioni, C. Sacchi, and C. Regazzoni, "Non-Gaussian characterization of DS/CDMA noise in few-user systems with complex signature sequences," *IEEE Trans. Signal Processing*, vol. 47, pp. 234–237, Jan. 1999.

[8] K. Huang, "Supplementary proof for "Exact and approximate construction of digital phase modulations by superposition of AMP" by P. A. Laurent," *IEEE Trans. Communications*, vol. 53, pp. 234–237, Feb. 2005.